AD-A190 518 TESTING FINITE DIFFERENCING SCHEMES FOR THE SHALLOW WATER EQUATIONS(U) SACLANT ASW RESEARCH CENTRE LA SPEZIA (ITALY) G PECCION OCT 87 SACLANTCEN-SM-202 1/1

UNCLASSIFIED F/G 8/3 NL

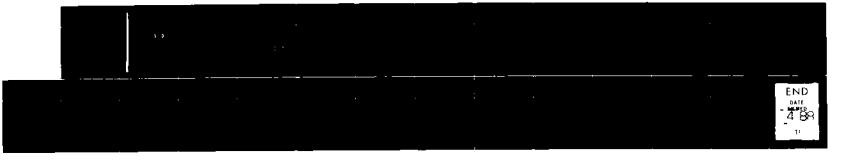

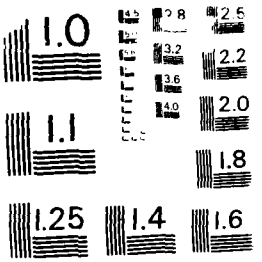

MICROCOPY RESOLUTION TEST CHA
NATIONAL BUREAU OF STANDARDS - 1963

(4)

DTIC FILE COPY

SACLANTCEN MEMORANDUM
serial no.: SM-202

SACLANT ASW
RESEARCH CENTRE
MEMORANDUM

AD-A190 518

DTIC
ELECTE
DEC 1 1 1987
S D
H

Testing finite differencing schemes for the shallow water equations

G. Peggion

October 1987

The SACLANT ASW Research Centre provides the Supreme Allied Commander Atlantic (SACLANT) with scientific and technical assistance under the terms of its NATO charter, which entered into force on 1 February 1963. Without prejudice to this main task—and under the policy direction of SACLANT—the Centre also renders scientific and technical assistance to the individual NATO nations.

DISTRIBUTION STATEMENT A
Approved for public release;
Distribution Unlimited

87

This document is released to a NATO Government at the direction of SACLANT ASW Research Centre subject to the following conditions:

- The recipient NATO Government agrees to *use its best endeavours to ensure* that the information herein disclosed, whether or not it bears a security classification, is not dealt with in any manner (a) contrary to the intent of the provisions of the Charter of the Centre, or (b) prejudicial to the rights of the owner thereof to obtain patent, copyright, or other like statutory protection therefor.

- If the technical information was originally released to the Centre by a NATO Government subject to restrictions clearly marked on this document the recipient NATO Government agrees to use its best endeavours to abide by the terms of the restrictions so imposed by the releasing Government.

Page count for SM-202
(excluding covers)

Pages	Total
i-iv	4
1-18	18
	22

SACLANT ASW Research Centre
Viale San Bartolomeo 400
19026 San Bartolomeo (SP), Italy

tel 0187 540 111
telex 271148 SACENT I

NORTH ATLANTIC TREATY ORGANIZATION

SACLANTCEN SM-202

Testing finite differencing schemes for the shallow water equations

G. Peggion

The content of this document pertains to work performed under Project 04 of the SACLANTCEN Programme of Work. The document has been approved for release by The Director, SACLANTCEN.

DTIC
SELECTE
DEC 1 1 1987
S
H

Issued by
Underwater Research Division

DTIC COPY INSPECTED 8

R. Thiele

R Thiele
Division Chief

Accession For
NTIS GRA&I
DTIC TAB
Unannounced
Justification
By per letter
Distribution/
Availability Codes
Dist Avail and/or Special
A-1

intentionally blank page

Testing finite differencing schemes for the shallow water equations

G. Peggion

Abstract: The explicit, the semi-implicit, and the fractional step schemes are tested and compared in the solution of the shallow water equations. The explicit finite-difference formulation is the most accurate, but is restricted by a stability condition which is not suitable for long-term numerical simulations. The standard semi-implicit scheme requires the solution of an elliptic equation which is also time-consuming. The fractional step method results in the least accurate, but computationally the most efficient solution.

Keywords: Courant-Friedrichs-Levy stability condition • explicit scheme • fractional step method • semi-implicit scheme • shallow water equation

Contents

1. Introduction

The study of ocean and atmosphere dynamics classically develops from setting mathematical frameworks. These may be collections of numbers labelled as observations or systems of equations, considered as 'truly representative' of the dynamics. Within the limits of the assumptions and approximations of the analytical model, the numerical technique used for solving the problem may introduce two additional distortions into the representation of the solutions: the error inherent from the truncated arithmetic and the error created by approximating continuous differential equations with discrete algebraic expressions (Grotjahn and O'Brien, 1976). However, the accuracy of the solutions is not the only requirement to be fulfilled in the development of ocean and atmosphere models. At the present stage of technology, computer efficiency might be an even more restrictive condition.

The shallow water equations are the prototype equations for primitive equation models of ocean/atmosphere dynamics. It is well known that numerical techniques based on explicit-time differencing schemes are considerably affected by the Courant-Friedrichs-Levy (CFL) stability condition that controls the high-frequency gravity wave motion. Although explicit schemes are always more accurate than implicit, the latter are widely applied because they are able to use much larger time steps (O'Brien, 1986). In general, fully-implicit schemes are seldom applied, and semi-implicit schemes are often applied in ocean/atmosphere models (Hamilton, 1977). Such schemes treat the terms that govern the fast gravity waves implicitly and the remainder explicitly.

The implicit/semi-implicit schemes usually require the solution of a two-dimensional Poisson or Helmholtz equation. A large number of different solver routines exist for such an elliptic equation. However, all these methods are time-consuming and most of them are applicable only for particular boundary shapes or boundary condition specifications. In order to avoid this problem, Tanguay and Robert (1986) have recently proposed an algorithm called the fractional step method, which reduces the matrix from the Helmholtz equation to a simple tridiagonal system in each of the two horizontal spatial dimensions. Consequently, solutions can be efficiently obtained by a special form of Gaussian elimination method (Carnahan et al., 1969). The practical advantage is that no additional computer time is required in this part of the calculations (compared to the total computation of large-scale dynamics models). Although the Tanguay-Robert algorithm is based on a modified version of the shallow water equations with the inclusion of an extra nonphysical term, the method looks so promising that the main purpose of this study is to verify the accuracy of the scheme in long-term numerical simulations. The scheme is therefore tested and compared with the explicit and the semi-implicit methods.

Section 2 presents the formulation of the different numerical schemes. The schemes are compared in Sect. 3, and the results discussed in Sect. 4.

2. The scheme formulations

2.1. THE CONTINUOUS AND DISCRETE SHALLOW WATER EQUATIONS

We consider a simplified formulation of the shallow water equations (Pedlosky, 1979). The equations are referred on a f-plane with a cartesian coordinate system (x, y) chosen such that in the Northern hemisphere the x-coordinate increases eastwards and the y-coordinate increases polewards, taking the form

$$u_t - f_0 v = -g\eta_x, \tag{2.1.1a}$$

$$v_t + f_0 u = -g\eta_y, \tag{2.1.1b}$$

$$\eta_t + H(u_x + v_y) = 0. \tag{2.1.1c}$$

The subscripts (x, y, t) denote partial differentiation; the variables (u, v) are the components of the eastward and poleward velocities, respectively. The variable η represents the free surface displacement, g is the gravitational acceleration, f_0 the Coriolis parameter, and H the total depth of the water column. Without a loss of generality we assume flat bottom topography. The equations are satisfied in the domain $D = \{(x, y) | 0 < x < L_x,\ 0 < y < L_y\}$.

The analytical solution of Eq. (2.1.1) may have the simple form

$$(u, v, \eta) = (U, V, N)e^{i(\omega t + \kappa x + \ell y)}, \tag{2.1.2}$$

where N is the amplitude of the wave, ω the frequency, and κ and ℓ the wavenumbers. It can be easily proved that the coefficients U and V as a function of amplitude are given by

$$U = -\frac{gN}{\omega^2 - f_0^2}(\kappa\omega - i\ell f_0), \qquad V = -\frac{gN}{\omega^2 - f_0^2}(\ell\omega + i\kappa f_0). \tag{2.1.3a}$$

The wave expressed by (2.1.2) satisfies the dispersion relationship

$$\omega = \sqrt{f_0^2 + gH\Theta^2}, \tag{2.1.3b}$$

and has a group velocity GV of components

$$\mathrm{GV} = \left(\frac{gH\kappa}{\sqrt{f_0^2 + gH\Theta^2}},\ \frac{gH\ell}{\sqrt{f_0^2 + gH\Theta^2}}\right), \tag{2.1.3c}$$

where $\Theta = \sqrt{\kappa^2 + \ell^2}$. Only positive frequency values are considered henceforth.

The analytical problem (2.1.1) is numerically approximated on a C-grid. We have chosen this grid because it is the one most often used in large-scale dynamical models (Grammeltvedt, 1969). All the terms are centred differences in space, with a grid network such that the functions u, v, and η have the numerical correspondent

$$\begin{aligned} u^n_{j,m} &= u((2j+1)\Delta x, 2m\Delta y, n\Delta t), \\ v^n_{j,m} &= v(2j\Delta x, (2m+1)\Delta y, n\Delta t), \\ \eta^n_{j,m} &= \eta(2j\Delta x, 2m\Delta y, n\Delta t), \end{aligned} \tag{2.1.4}$$

where j, m and n are the indices relative to the variables x, y and t, respectively. However, we will suppress the indices when not incremented. With the above assumptions and notations, the solution (2.1.1) is discretized as follows:

$$u = U_* e^{i(\phi_* + \kappa\Delta x)}, \qquad v = V_* e^{i(\phi_* + \ell\Delta y)}, \qquad \eta = N e^{i\phi_*},$$

$$\phi_* = \phi^n_{j,m} = \omega_* n\Delta t + \kappa 2j\Delta x + \ell 2m\Delta y, \tag{2.1.5}$$

where $*$ indicates values to be computed for different schemes. The schemes are illustrated in the following sections.

2.2. THE EXPLICIT SCHEME

With the explicit scheme, Eqs. (2.1.1) are written as follows:

$$u^{n+1} = u^{n-1} + 2f_0\Delta t[v]^n - \frac{g\Delta t}{\Delta x}(\eta_{j+1} - \eta_j)^n, \tag{2.2.1a}$$

$$v^{n+1} = v^{n-1} - 2f_0\Delta t[u]^n - \frac{g\Delta t}{\Delta y}(\eta_{m+1} - \eta_m)^n, \tag{2.2.1b}$$

$$\eta^{n+1} = \eta^{n-1} - H\Delta t\left(\frac{u_j - u_{j-1}}{\Delta x} + \frac{v_m - v_{m-1}}{\Delta y}\right)^n, \tag{2.2.1c}$$

where $[\ldots]$ indicates the average over the four closest points.

This scheme is affected by the CFL stability condition, which requires a time step Δt such that

$$\Delta t^2\left[f_0^2 + gH\left(\frac{1}{\Delta x^2} + \frac{1}{\Delta y^2}\right)\right] \leq 1. \tag{2.2.2}$$

Relative to the solutions (2.1.5), the scheme gives the following values:

$$U_E = \frac{gN}{\Xi_E^2 - \Lambda^2}\left(\Xi_E \frac{\sin\kappa\Delta x}{\Delta x} - i\Lambda\frac{\sin\ell\Delta y}{\Delta y}\right),$$

$$V_E = \frac{gN}{\Xi_E^2 - \Lambda^2}\left(\Xi_E \frac{\sin\ell\Delta y}{\Delta y} + i\Lambda\frac{\sin\kappa\Delta x}{\Delta x}\right), \tag{2.2.3a}$$

$$\omega_E = \frac{1}{\Delta t}\arcsin\left(\Delta t\sqrt{\Lambda^2 + \Gamma^2}\right) \tag{2.2.3b}$$

where

$$\Lambda = f_0 \cos\kappa\Delta x \cos\ell\Delta y,$$

$$\Gamma = \sqrt{gH\left(\frac{\sin^2\kappa\Delta x}{\Delta x^2} + \frac{\sin^2\ell\Delta y}{\Delta y^2}\right)},$$

$$\Xi_E = \frac{\sin\omega_E\Delta t}{\Delta t}. \tag{2.2.3c}$$

The components of the vector group velocity are symmetric, so we will consider only one of them, namely the eastward component. Unfortunately, the mathematical representation of the computational group velocities might be quite complex, and although intriguing would add no significant information about the associated numerical distortions. Thus it is only the group velocity values for non-rotational flows (viz. $f_0 = 0$) that are presented henceforth:

$$GV_E = \frac{gH}{\Gamma\sqrt{1 - \Delta t^2\Gamma^2}} \cdot \frac{\sin 2\kappa\Delta x}{2\Delta x}. \tag{2.2.3d}$$

We recognize a formal similarity between Eqs. (2.2.3) and (2.1.3) in the sense there are the 'computational wavenumbers' $\sin\kappa\Delta x/\Delta x$ and $\sin\ell\Delta y/\Delta y$ corresponding to the 'true wavenumbers' κ and ℓ, and the 'computational Coriolis frequency' Λ corresponding to the 'true Coriolis parameter', f_0. These computational terms are independent of the explicit treatment of the Eq. (2.1.1). They are a direct consequence of the centred-in-space finite difference approximation, and the C-grid (i.e. the 4-point average), respectively. Besides these computational variables, there are the additional computational frequencies, Ξ_E, and ω_E. While the frequency Ξ_E is the result of the centred-in-space finite difference scheme, the frequency ω_E is intrinsic the explicit formulation. Thus we take ω_E to be the effective 'computational phase frequency' of the explicit scheme.

It is easy to verify that all the computational variables converge and will converge to the corresponding analytical values as the increments Δt, Δx, and Δy tend to zero.

It generally follows that the representation is fairly good for long waves (i.e. those resolved by several grid points), but poor for shorter waves, particularly those with wavelengths less than $4\Delta x$, $4\Delta y$ a wavelength $4\Delta x$ corresponds to $\kappa\Delta x = \pi/2$ (Grotjahn and O'Brien, 1976).

2.3. THE SEMI-IMPLICIT SCHEME

The semi-implicit treatment of the shallow water equations is written as follows:

$$\begin{aligned}
\delta_t u^n &= -\tfrac{1}{2} g(\delta_x \eta^{n+1} + \delta_x \eta^n) + f_0 [v]^n, \\
\delta_t v^n &= -\tfrac{1}{2} g(\delta_y \eta^{n+1} + \delta_y \eta^n) - f_0 [u]^n, \\
\delta_t \eta^n &= -\tfrac{1}{2} H(\delta_x u^{n+1} + \delta_x u^n + \delta_y v^{n+1} + \delta_y v^n),
\end{aligned} \tag{2.3.1}$$

where δ_t, and δ_x, δ_y are the centered finite difference operators in time and space respectively. With the use of incremented index variables, Eq. (2.3.1) are written as

$$u^{n+1} + \frac{g\Delta t}{2\Delta x}(\eta_{j+1} - \eta_j)^{n+1} = Q1, \tag{2.3.2a}$$

$$v^{n+1} + \frac{g\Delta t}{2\Delta x}(\eta_{m+1} - \eta_m)^{n+1} = Q2, \tag{2.3.2b}$$

$$\eta^{n+1} + \frac{H\Delta t}{2\Delta x}(u_j - u_{j-1})^{n+1} + \frac{H\Delta t}{2\Delta y}(v_m - v_{m-1})^{n+1} = Q3, \tag{2.3.2c}$$

where $Q1$, $Q2$, and $Q3$ contain the remaining terms evaluated at time step n or $n-1$. Substitution of (2.3.2a)-(2.3.2b) into (2.3.2c) leads to the numerical Helmholtz equation for η^{n+1}, when all the variables at time step n are known:

$$-a\eta_{j+1} - a\eta_{j-1} - b\eta_{m+1} - b\eta_{m-1} + (1 + 2a + 2b)\eta = Q, \tag{2.3.2d}$$

where

$$a = \frac{gH\Delta t^2}{4\Delta x^2}, \qquad b = \frac{gH\Delta t^2}{4\Delta y^2}. \tag{2.3.2e}$$

Once the surface elevations are determined, the velocity field can be updated from Eqs. (2.3.2a)-(2.3.2b). The scheme is still affected by the CFL stability condition

$$f_0 \Delta t < 1$$

With respect to the analytical solution of (2.1.1), the scheme gives the following computational values:

$$U_{SI} = \frac{gN\cos(\omega_{SI}\Delta t)}{\Xi_{SI}^2 - \Lambda^2}\left(\Xi_{SI}\frac{\sin\kappa\Delta x}{\Delta x} - i\Lambda\frac{\sin\ell\Delta y}{\Delta y}\right),$$

$$U_{sI} = \frac{gN\cos(\omega_{sI}\Delta t)}{\Xi_{sI}^2 - \Lambda^2}\left(\Xi_{sI}\frac{\sin\ell\Delta y}{\Delta y} + i\Lambda\frac{\sin\kappa\Delta x}{\Delta x}\Lambda\right), \tag{2.3.3a}$$

$$\omega_{sI} = \frac{1}{\Delta t}\arctan\left(\Delta t\sqrt{\Lambda^2 + \Gamma^2}\right), \tag{2.3.3b}$$

$$GV_{sI} = \frac{gH}{\Gamma(1 + \Delta t^2\Gamma^2)}\frac{\sin 2\kappa\Delta x}{2\Delta x}, \tag{2.3.3c}$$

where Ξ_{sI} is formally identical to Ξ_I.

A formal comparison between Eqs. (2.3.3) and (2.1.3) indicates that the semi-implicit scheme affects the amplitude of the wave, introducing also a 'computational amplitude' $N_{sI} = N\cos(\omega_{sI}\Delta t)$. Thus, the semi-implicit scheme tends to underestimate both frequency and amplitude of the waves.

2.4 THE FRACTIONAL-STEP METHOD

In order to factorize the Helmholtz Eq. (2.3.2a), the fractional step method substitutes the continuity Eq. (2.1.1c) with

$$\eta + M(u_x + v_y) = 0, \tag{2.4.1a}$$

where

$$M = (gH\Delta t^2)^2\frac{\partial^4\eta}{\partial x^2\partial y^2}. \tag{2.4.1b}$$

Treating the Eqs. (2.1.1a,b,c) and (2.4.1) semi-implicitly, the η-equation (2.3.2a) takes the form

$$\mathcal{L}(\eta) = \mathcal{L}_x\mathcal{L}_y(\eta) = (1 - gH\Delta t^2\delta_x^2)(1 - gH\Delta t^2\delta_y^2)\eta = Q + \mu^{n-1}, \tag{2.4.2}$$

where $\mathcal{L}_x$ and $\mathcal{L}_y$ are the second order centered difference operators on x and y, respectively, and $\mu = (gH\Delta t^2)^2\delta_x^2\delta_y^2\eta$. Since the term μ is of fourth order in Δt, the scheme should not introduce any significant error in the solution (Flanguay and Robert, 1986).

The computational values associated to the scheme are

$$U_F = \frac{gN\cos(\omega_F\Delta t)}{\Xi_F^2 - \Lambda^2}\left(\Xi_F\frac{\sin\kappa\Delta x}{\Delta x} - i\Lambda\frac{\sin\ell\Delta y}{\Delta y}\right),$$

$$V_F = \frac{gN\cos(\omega_F\Delta t)}{\Xi_F^2 - \Lambda^2}\left(\Xi_F\frac{\sin\ell\Delta y}{\Delta y} + i\Lambda\frac{\sin\kappa\Delta x}{\Delta x}\right), \tag{2.4.3a}$$

$$\omega_F = \frac{1}{\Delta t}\arctan\left(\Delta t\sqrt{\frac{\Lambda^2(1+\Delta t^2\alpha^2)+\Gamma^2}{(1+\Delta t^2\alpha^2)(1-\Delta t^2\Lambda^2)}}\right), \tag{2.4.3b}$$

$$GV_F = \sqrt{1+\Delta t^2\alpha^2}\left(\frac{gH\sin 2\kappa\Delta x}{\Gamma-2\Delta x}\frac{\Gamma\alpha}{1+\Delta t^2\alpha^2}\frac{\sin f\Delta y}{\Delta y}\Delta t^3 gH\cos\kappa\Delta x\right), \tag{2.4.3c}$$

where

$$\alpha = gH\Delta t\frac{\sin\kappa\Delta x}{\Delta x}\frac{\sin f\Delta y}{\Delta y} \tag{2.4.3d}$$

It is easy to verify that the fractional step computational variables converge to the semi-implicit computational variables as $O(\Delta t^4)$. Therefore for small Δt increments the two schemes should end up virtually identical, confirming the Tanguay and Robert (1986) hypothesis.

The x- and y-symmetry of the operator $\mathcal{L}$ of (2.4.2) suggests the solution of the η-equation using an alternating direction iterative algorithm in which the x- and y-operators are inverted at each time step. At each iteration only the boundary conditions at two opposite sides are necessary. Let us solve the operator (2.4.2) with the following algorithm.

First, we compute $v_{j,m}$ from

$$\mathcal{L}_x v = (1-gH\Delta t^2\delta_x^2)v = Q+\mu^{n-1} \tag{2.4.4a}$$

at the inner η mesh points; no boundary conditions are required at this stage except for the terms that appear in the righthand side of (2.4.2). Now we compute $\eta_{j,m}^{n+1}$ from

$$\mathcal{L}_y\eta = (1-gH\Delta t^2\delta_y^2)\eta = v \tag{2.4.4b}$$

using only the boundary conditions at the northern and southern boundaries. At the following time step the operator $\mathcal{L}_x$, and $\mathcal{L}_y$ are inverted. Subsequently, the use of an alternating direction algorithm allows a more accurate application of all the boundary conditions.

3. Applications

To verify the accuracy of the schemes fully we now compare numerical results with exact analytical solutions of problem (2.1.1). Numerical experiments are performed with the following common features: total depth $H = 2000$ m, total extensions $L_x = 1000$ km, and $L_y = 1000$ km, and grid spacing $\Delta x = 17.4$ km, $\Delta y = 17.4$ km. Although the formulas presented in the previous sections are formally symmetric with respect to the wavenumbers κ and ℓ, there is a different structure to the errors because they contain quadratic terms. Nevertheless, the computational frequencies and group velocities of the schemes are depicted in a one-dimensional form in Figs. 1–3. For simplicity we consider irrotational flows (*i.e.* $f_0 = 0$) and choose the wavenumbers such that $\kappa\Delta x = \ell\Delta y$. The schemes are tested for various values of the non-dimensionalized ratio

$$\tau = \sqrt{gH}\,\frac{\Delta t}{\sqrt{2}\Delta x},$$

Grotjahn and O'Brien (1976) gave an accurate and complete analysis of the distortions introduced by the explicit and semi-implicit time differencing schemes. In general, explicit formulations have the tendency to overestimate the oscillations, whereas the implicit have the tendency to underestimate. Although explicit schemes are found to be more accurate than the implicit, the accuracy is usually incommensurate with the higher computational cost. The same findings apply to the fractional step method. As Fig. 3 confirms, the fractional step method introduces the same distortions of the semi-implicit approximation, but it is slightly less accurate. However the errors might well be compensated for the increased computational efficiency.

Finally we compare the solutions obtained by solving numerically the problem (2.1.1) with the exact solution

$$(u, v, \eta) = (U, V, N)\sin(\omega_0 t + \kappa_0(x + y)),$$

where the wavenumber is $\kappa_0 = 7.88 \times 10^{-8}$ cm^{-1}, and the frequency is $\omega_0 = 1.44 \times 10^{-3}$ s^{-1}. The amplitude is $N = 20$ cm, the velocities U and V are defined as in (2.1.3a). The wavenumber κ_0 corresponds to a wavelength $\lambda = 50$ in terms of the grid intervals. To obtain a good resolution of the wave period, the implicit schemes used a time step $\Delta t = 217$ s, which implies 20 time-iterations per period, and a value $\tau \sim 1.25$ The explicit scheme employ a time step $\Delta t = 50$ s, corresponding to a value $\tau \sim 0.3$.

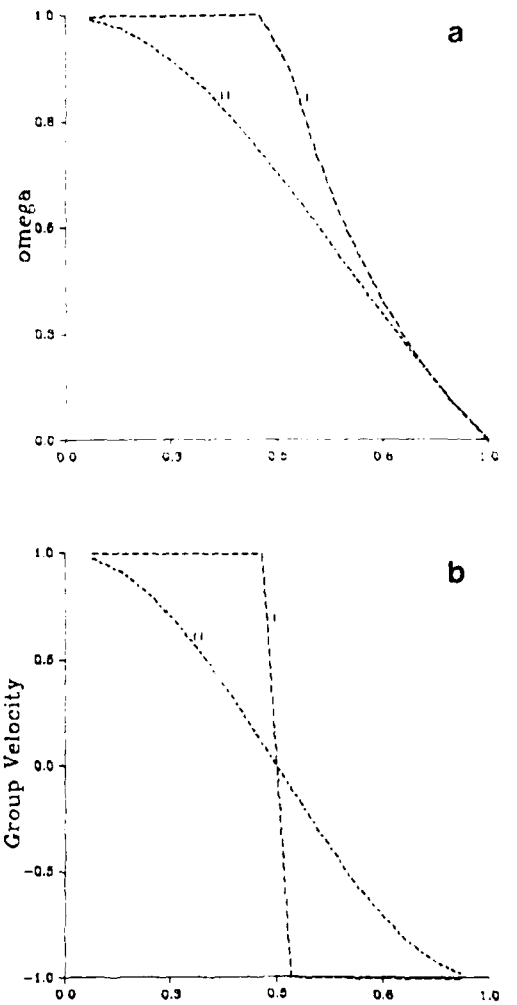

Fig. 1: The computational frequency (a) and computational group velocity (b) of the explicit scheme normalized by the analytical exact value. The abscissa represents the variable $\kappa\Delta x$ normalized by π. (I) $r = 0.01$, or $\Delta t = 1.75$; (II) $r = 0.5$ or $\Delta t = 87$.

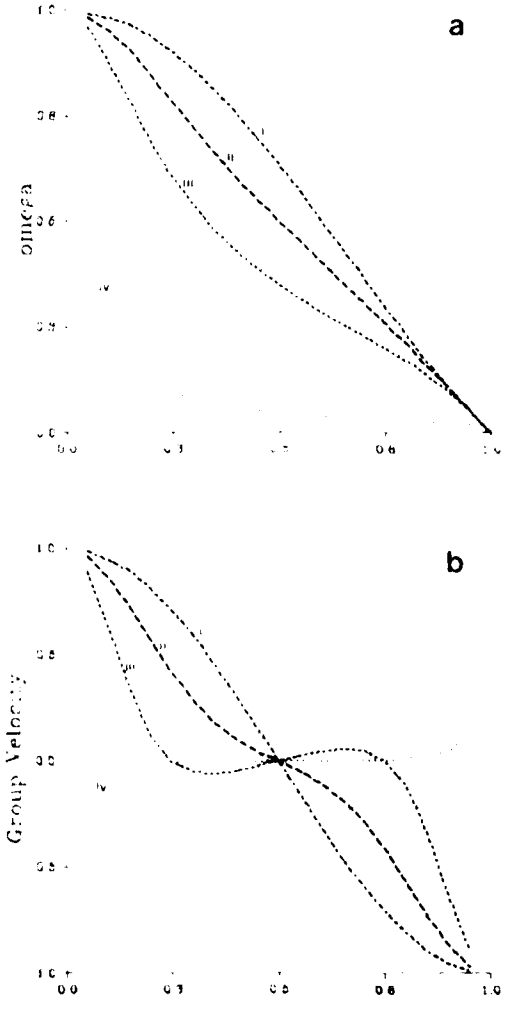

Fig. 2 The computational frequency (a) and computational group velocity (b) of the semi-implicit scheme: (I) $\tau = 0.01$ or $\Delta t = 1.75$; (II) $\tau = 0.5$ or $\Delta t = 87.$; (III) $\tau = 1$ or $\Delta t = 175$; (IV) $\tau = 10$ or $\Delta t = 1750$.

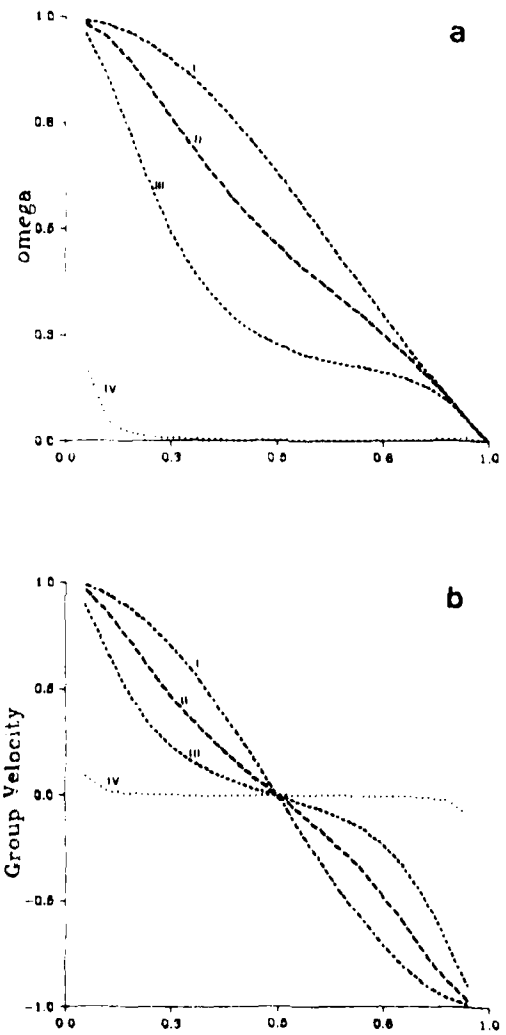

Fig 3 The computational frequency (a), and computational group velocity (b) of the fractional step method. Same as Fig 2.

Because of the staggered C grid, the numerical algorithms require knowledge of the surface elevation at all the lateral boundaries and of the Coriolis terms fav and fau at the north-south and east-west boundaries respectively. In order to reduce the distortion due to the treatment of the boundary conditions, we force the schemes by specifying the boundary conditions from the exact analytical values. The use of the leapfrog scheme in time requires knowledge of all the variables at two initial time steps. Tests have been made to ensure that the given initial conditions do not affect the evolution of the solution. No substantial differences have been found after the initial adjustment, which is of the order of 1 period. In the following experiments, the algorithms are initialized with exact values at two consecutive time steps.

The evolution of the sea surface displacement at the middle point of the basin is depicted in Fig. 4. It follows that the explicit scheme is definitely the most precise, with virtually no errors. On the other hand, of the implicit approximations, it is the semi-implicit scheme that is the most accurate. But the differences are minimal with respect to the total distortion.

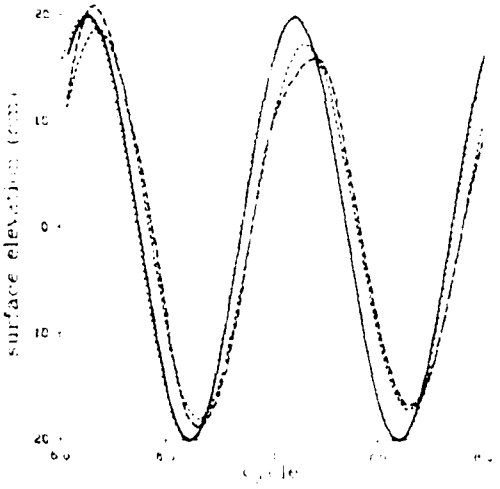

Fig. 4 The evolution of the free surface displacement at the middle point of the basin: (a) explicit scheme, (b) semi-implicit scheme, (c) fractional step method. The solid line represents the analytical solution.

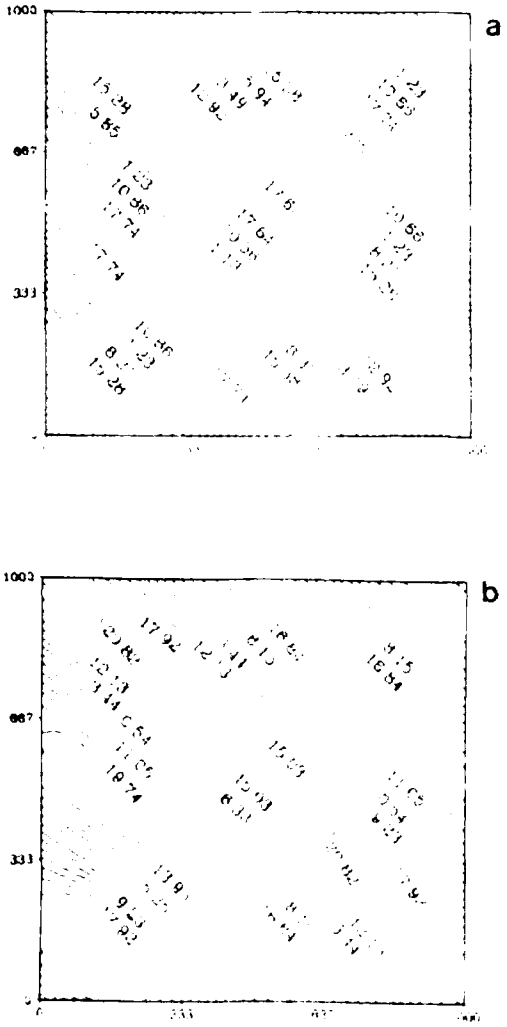

Fig. 5. The horizontal distribution of the free surface displacement after 5 wave periods. (a) explicit scheme (b) semi-implicit scheme. (c) analytical solution.

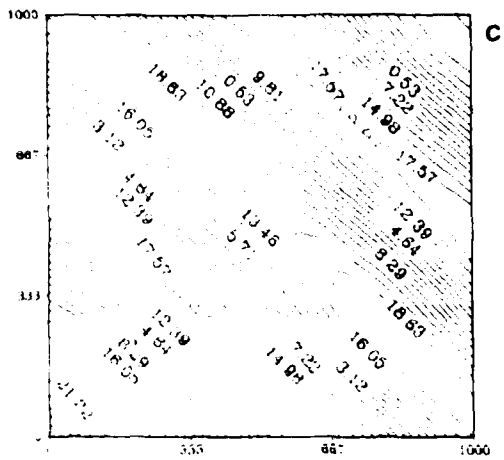

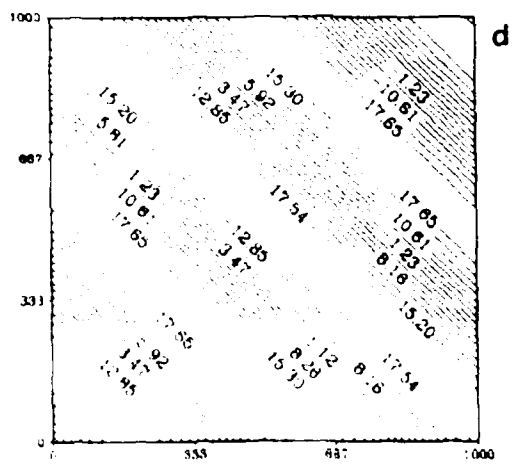

Fig. [illegible]

Figure 5 illustrates the surface elevation distribution over the whole basin after 8 wave periods. It is evident that specification of the boundary conditions together with the distortion between computational frequency (i.e. the frequency of the interior) and exact frequency (i.e. the frequency at the boundaries) affects the quality of the solution. In general all the numerical schemes are sensible to this problem. High frequency waves that are present at the boundaries, might be removed by transforming the boundary conditions into a forcing term for the η equation. This could be achieved by introducing a new function $\eta' = \eta - g(x, y, t)$, where g is an arbitrarily chosen high-frequency function such that $\eta' = 0$ on $\partial\Omega$, and solving the differential problem for η'. In this a way the solution is locally adjusted to the short waves, and the distortions between computational and exact frequencies are notably reduced.

4. Conclusion

[illegible] has been shown that several alternative numerical [illegible] the shallow water equations. Explicit schemes are [illegible] computationally the least efficient. For large time steps [illegible] stability by slowing the waves. Generally it is [illegible] handled reasonably well. Among the schemes not affected by the CFL stability condition, the fractional step method presents many advantages [illegible] easier, and the scheme is computationally more efficient [illegible] boundary [illegible] and boundary condition specifications.

Large scale dynamics ocean atmosphere models might be [illegible] boundary conditions, expecially in cases where boundary limits and boundary [illegible] are externally imposed, rather than directly defined from physical constraints. In this regard appropriate application of the alternating [illegible] direction iterative algorithms of the fractional step method might reduce the [illegible] propagating from the boundary to the interior.

[illegible] overall conclusion is that in terms of accuracy [illegible] range of applications, the fractional step method [illegible] large scale dynamics models.

References

CARNAHAN, B., LUTHER, H.A. and WILKES, J.O. *Applied numerical models*. New York, NY, Wiley, 1969.

GRAMMELTVEDT, A. A survey of finite schemes for the primitive equations for a barotropic fluid. *Monthly Weather Review*, **97**, 1969, 384–404.

GROTJAHN, R. and O'BRIEN, J.J. Some inaccuracies in finite differencing hyperbolic equations. *Monthly Weather Review*, **104**, 1976, 180–194.

HAMILTON, P. On the numerical formulation of a time-dependent multi-level model of an estuary, with particular reference to boundary conditions. *In*: Wiley, M., *ed*. Estuarine Processes II. New York, NY, Academic Press, 1977, 347–364.

O'BRIEN, J.J. *Advanced Physical Oceanographic Numerical Modelling*. NATO ASI Series, D. Dordrecht, Holland, Reidel, 1986.

PEDLOSKY, J. *Geophysical Fluid Dynamics*. New York, NY, Springs, 1979.

TANGUAY, M. and ROBERT, A. Elimination of the Helmholtz equation associated with the semi-implicit scheme in a grid point model of the shallow water equation. *Monthly Weather Review*, **114**, 1986, 2154–2162.

Initial Distribution for SM-202

Ministries of Defence	
JSPHQ Belgium	2
DND Canada	10
CHOD Denmark	8
MOD France	8
MOD Germany	15
MOD Greece	11
MOD Italy	10
MOD Netherlands	12
CHOD Norway	10
MOD Portugal	2
MOD Spain	2
MOD Turkey	5
MOD UK	20
SECDEF US	68

NATO Authorities	
Defence Planning Committee	3
NAMILCOM	2
SACLANT	10
SACLANTREPEUR	1
CINCWESTLANT/ COMOCEANLANT	1
COMSTRIKFLTANT	1
CINCIBERLANT	1
CINCEASTLANT	1
COMSUBACLANT	1
COMMAIREASTLANT	1
SACEUR	2
CINCNORTH	1
CINCSOUTH	1
COMNAVSOUTH	1
COMSTRIKFORSOUTH	1
COMEDCENT	1
COMMARAIRMED	1
CINCHAN	3

SCNR for SACLANTCEN	
SCNR Belgium	1
SCNR Canada	1
SCNR Denmark	1
SCNR Germany	1
SCNR Greece	1
SCNR Italy	1
SCNR Netherlands	1
SCNR Norway	1
SCNR Portugal	1
SCNR Turkey	1
SCNR UK	1
SCNR US	2
SECGEN Rep SCNR	1
NAMILCOM Rep SCNR	1

National Liaison Officers	
NLO Canada	1
NLO Denmark	1
NLO Germany	1
NLO Italy	1
NLO UK	1
NLO US	1

NLR to SACLANT	
NLR Belgium	1
NLR Canada	1
NLR Denmark	1
NLR Germany	1
NLR Greece	1
NLR Italy	1
NLR Netherlands	1
NLR Norway	1
NLR Portugal	1
NLR Turkey	1
NLR UK	1

Total external distribution	248
SACLANTCEN Library	10
Stock	22
Total number of copies	280

END

DATE

FILMED

4 88

DTIC